JOURNAL OF GEOPHYSICAL RESEARCH, VOL. 105, NO. A4, PAGES 7775-7782, APRIL 1, 2000

Io encounters past and present: A heavy ion comparison

C. M. S. Cohen, T. L. Garrard, and E. C. Stone
Space Radiation Laboratory, California Institute of Technology, Pasadena

J. F. Cooper
Hughes STX Corporation, Lanham, Maryland

N. Murphy
Jet Propulsion Laboratory, NASA, Pasadena, California

N. Gehrels
Goddard Space Flight Center, NASA, Greenbelt, Maryland

Abstract. The heavy ion counter (HIC) on the Galileo spacecraft consists of two low-energy telescopes that were proof-test models of the telescopes used for the cosmic ray subsystem (CRS) on Voyager. The telescopes on HIC were improved to better withstand the intense radiation environment of the Jovian system and to measure higher-energy particles with greater sensitivity. The similarity of these two instruments makes it natural to compare the data in an effort to glean insight on the behavior of heavy ion fluxes at higher energies and how the inner Jovian magnetosphere has changed in the last 18 years. Inside $L = 6$, the oxygen spectrum suggests a spectral break at ~ 7500 MeV/Gauss, corresponding to ions with gyroradii of ~ 1.5 R_{Io} at $L = 6$. A comparison of the phase space densities show remarkable agreement between the two time periods outside of the Io orbit, with differential spectra consistent with $\gamma \sim -8$ above ~ 6 MeV/nucleon. Near Io Galileo observed a large density gradient not apparent in the Voyager data that may be due to local time asymmetries or a decrease in the radial diffusion rate.

1. Introduction

The Voyager passages through the Jovian magnetosphere revealed an energetic heavy ion composition that differs substantially from that of the solar wind and interplanetary medium [*Krimigis et al.*, 1979a, b; *Vogt et al.*, 1979a, b]. The source of the observed dominant fluxes of oxygen and sulfur as well as the smaller amounts of sodium is the Io torus. The spatial and energetic distribution of heavy ions of energies greater than 1 MeV/nucleon were measured by two of the low-energy telescopes (LETs) comprising the cosmic ray subsystem (CRS). The measurements disclosed very steep energy spectra with power law indices of ~ 6 - 7 at energies between 8 and 15 MeV/nucleon. Data obtained at different radial distances allowed phase space density gradients to be determined and illustrated significant particle loss occurring between 5 and 12 R_J [*Gehrels et al.* 1981; *Gehrels and Stone* 1983]. Since the Voyager-1 encounter was brief and Voyager 2 did not pass inside 10 R_J, the temporal dependence of the particle loss could not be studied. Limited statistics prevented the characterization of the spectra at energies greater than 15 MeV/nucleon and the determination of phase space densities inside $L \sim 10$ for high magnetic moments.

Paper number 1999JA000021.
0148-0227/00/1999JA000021$09.00

In 1989, Galileo was launched to study the Jovian system in more detail. An encounter with Io was planned for the first orbit when the spacecraft entered the Jovian system in December 1995. The heavy ion counter (HIC) on Galileo is composed of two proof-test models of the CRS LETs, modified to enhance operation in the Jovian radiation environment, which makes a comparison of the Voyager 1 and Galileo data sets natural. The improvements made to HIC allow the CRS energy spectra to be extended to ~ 50 MeV/nucleon and the phase space density gradients over a larger L range for several magnetic moments to be determined. A comparison of the observations made over common magnetic moment intervals can begin to address long-term temporal changes in the particle flux which is sensitive to changes in the Io plasma torus density, diffusion rates, and scattering timescales. The CRS data used for this comparison were presented by *Gehrels et al.* [1981] and *Gehrels and Stone* [1983], and in this paper we concentrate on a comparison of the oxygen and sulfur spectra in the inner magnetosphere ($L \leq 8$).

2. Instrumentation

The low-energy telescopes (LETs) are standard dE/dx versus residual energy instruments using a series of solid state detectors to make measurements over a broad energy range. On CRS the LETs cover an energy range of ~ 1 - 25 MeV/nucleon, while on HIC, the combined energy range of the two LETs is ~ 6 - 200 MeV/nucleon. One of the two HIC

LETs (LET E) has thicker detectors optimized for nuclei with energies of 15-200 MeV/nucleon with a thick window that shields the detectors from low-energy protons. Although this also excludes lower-energy oxygen and sulfur ions, these ions are measured by the second HIC LET (LET B) that has a thinner window and a threshold of 6 MeV/nucleon in the normal operating mode (three-detector coincidence and one anticoincidence detector). When one or two detectors are deleted from the coincidence requirement, the threshold is reduced to 4 and 2.4 MeV/nucleon, respectively. This was done at consecutive intervals during the Io flyby on December 7, 1995. The electronic thresholds on individual HIC detectors are also substantially higher than on CRS to reduce the counting rate due to the large trapped proton flux. The HIC geometry factor is larger by a factor of 10 (in certain modes), allowing much lower fluxes to be measured. More detailed descriptions of HIC and CRS are given by *Garrard et al.* [1992] and *Stone et al.* [1977], respectively.

3. Observations

The HIC results reported here were accumulated during the Io orbit passage on December 7 - 8, 1995. Figure 1a shows the LET B count rate for this interval as a function of L. The gaps in the counting rate correspond to changes in the detector coincidence mode, with the highest rate occurring when only the front (LB 1) detector, with a 2.4 MeV/nucleon threshold, was required and lower rates resulting from the double (4 MeV/nucleon) and triple (6 MeV/nucleon) coincidence modes. The lowest threshold was maintained during closest approach to Io and resulted in a well-defined "microsignature" to be discussed in future work. The changes in count rates at each shift in the coincidence requirement indicate an approximate spectral index of ~ 2.5 for the integral flux spectrum at 2.4 - 6 MeV/nucleon, considerably harder than found at higher energies with LET E, as will be discussed later.

Figure 1b shows the spin averaged count rate profile of the first LET E detector (LE 1) for the same time period. The data were obtained over two time periods separated by 5 hours, the first occurring while Galileo was inbound and covering an L range of 8 - 5.4 and the second being outbound and corresponding to $5.4 > L > 4.4$ (the LET B sensor was turned off during this second time period). These data were divided into three regions for analysis: (1) radially outside the macrosignature (centered around 5.9 R_J), (2) spanning it, and

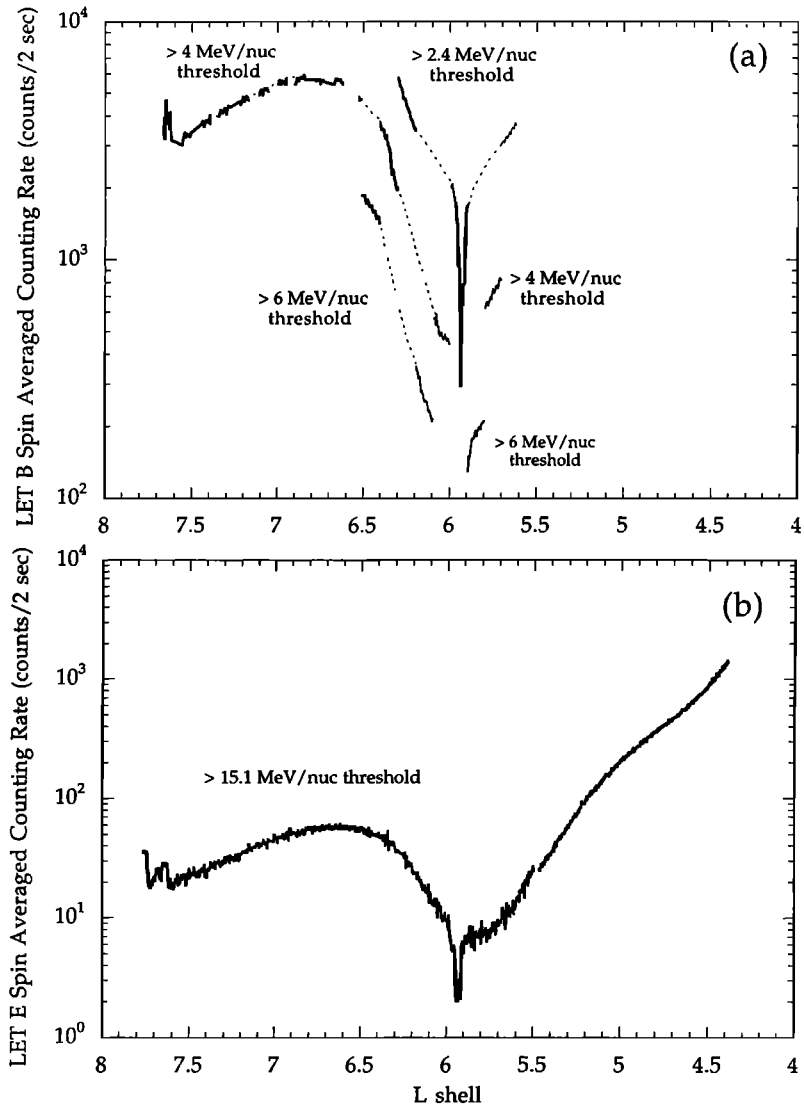

Figure 1. (a) Low-energy telescope (LET) B and (b) LET E spin-averaged singles rate versus radial distance for Io encounter. The dashed curves in the gaps in the data are to guide the eye.

(3) radially inside. The boundaries of these regions, placed at L values of ~ 6.6 and 5.0, were subjective estimates of where particle losses due to Io (whose position varies from $L = 5.9$ to 6.9) begin to dominate over losses most likely due to pitch angle scattering [*Gehrels*, 1982]. Within each region the data were further divided into ~ 1 hour long time periods (subregions 1a, 1b, 2a, 2b, 2c, 3a, 3b). Such long averaging times were necessary due to the limited statistics. The times, average L shell, L shell range and spacecraft and equatorial magnetic field magnitudes (estimated from a model by A. Cheng and C. Paranicas, private communication, 1996) for each subregion are given in Table 1.

For each LET E event the nuclear charge Z was calculated, and evident background was subtracted. Those events with an estimated Z within given ranges were classified as oxygen or sulfur. Figure 2 illustrates these ranges for region 1. Incident energy was determined from the total energy deposited by the ion in the telescope and the counts were converted into a flux using a response matrix which characterizes LET E.

4. Energy Spectra

The oxygen spectra for each subregion are presented in Figure 3. Spectral indices of power law fits to the data are given in Table 2. From Figure 3 it is apparent that as the particles diffuse inward toward Io's orbit (L ~ 5.9), there is a slight softening of the spectrum, as would be expected due to strong pitch angle scattering believed to be occurring at $L > 6$ [*Thorne*, 1982]. When the particles have passed Io, the spectrum becomes much softer with the suggestion of a spectral break around 7500 MeV/Gauss. The dramatic change in the spectral index from L = 6.4-5.8 at magnetic moments above 7500 MeV/Gauss supports the conclusion that the diffusion time increases by an order of magnitude near $L = 6$ [c.f. Figure 10, *Gehrels and Stone* [1983] and *Siscoe et al.* [1981]]. Such an increase allows more time for scattering and results in a greater loss of particles with larger magnetic moments, softening the spectrum. Inside $L = 5.8$, the spectra above the 7500 MeV/Gauss harden with decreasing L, indicating that pitch angle scattering at the strong scattering limit is not the dominant loss process inside Io, as this would soften the spectra. However, it is evident from the decrease in differential flux between $L = 5.8$ and 5.3 that there is pitch angle scattering occurring, resulting in a substantial particle loss in this region. Since the phase space density is inversely related to the flux by a factor of B^2, which increases with decreasing radial distance, one expects a large positive radial gradient in density to be determined from these data. This is the case and will be discussed in more detail in section 5.

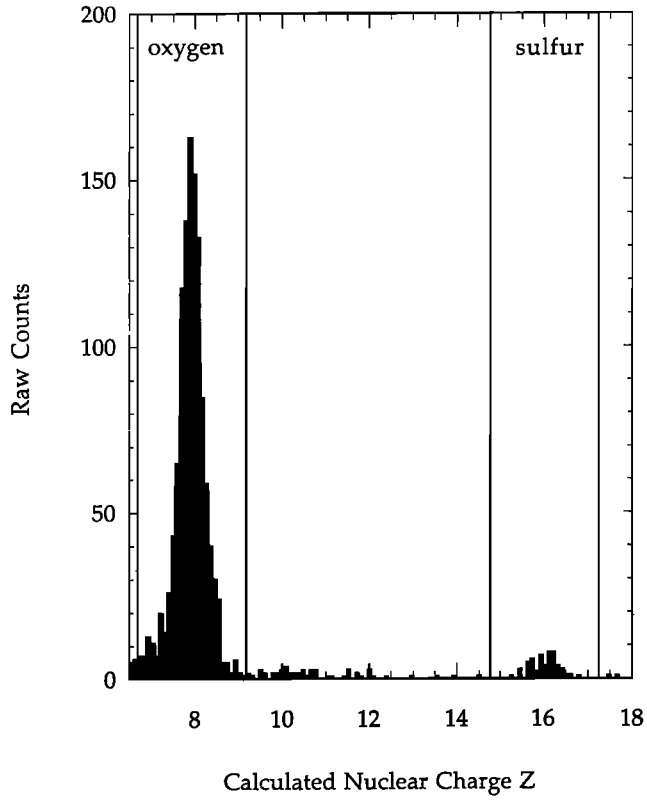

Figure 2. LET E events (with energies greater than 15 MeV/nucleon) from region 1. The two Z ranges denote events that were classified as either oxygen or sulfur.

The presence and position of the spectral break in the spectrum at $L = 4.5$ corresponds to oxygen ions with gyroradii of ~ 1.5 R_{Io} at $L = 6$ and is possibly indicative of Io's influence on the flux of heavy ions. That the spectrum is harder below the break than above is consistent with Io preferentially absorbing ions with smaller gyroradii and not significantly affecting those with gyroradii greater than ~ 1.5 R_{Io}. This is supported by the significant reduction in C/O inside Io's orbit compared to outside Io's orbit reported by *Garrard et al.* [1996]. Carbon, which originates from the solar wind, is nearly fully stripped and has a much smaller gyroradius than oxygen, which is predominantly Iogenic and singly charged [*Barbosa et al.*, 1984; *Hamilton et al.*, 1992].

Spectra from subregions 1a and 2c were obtained at comparable distances to spectra presented by *Gehrels and Stone* [1983]. In Figure 4 it can be seen that the differential spectrum ($E^{-7.9\pm0.3}$) for $E \geq 14$ MeV/nucleon is consistent within the uncertainties with the fit ($E^{-7.0\pm2.6}$) to the Voyager

Table 1. Subregion Characteristics

Subregion	Start Time	Stop Time	<R>	<B>*	<B_0>*	L Range*	<L>*
1a	341 1521	341 1603	7.4	0.0109	0.0101	7.22 - 7.76	7.5
1b	341 1603	341 1645	6.9	0.0133	0.0127	6.68 - 7.22	7.0
2a	341 1645	341 1735	6.3	0.0168	0.0165	6.06 - 6.68	6.4
2b	341 1735	341 1826	5.7	0.0222	0.0221	5.49 - 6.06	5.8
2c	342 0050	342 0126	5.3	0.0294	0.0288	5.11 - 5.47	5.3
3a	342 0006	342 0050	4.9	0.0366	0.0359	4.72 - 5.11	4.9
3b	341 2322	342 0006	4.4	0.0468	0.0462	4.39 - 4.72	4.5

* Determined from model by A. Cheng and C. Paranicas (private communication, 1996).

Table 2. Subregion Oxygen Spectral Indices

L Value	Magnetic Moment (MeV/Gauss)	Oxygen Differential Spectral Index
7.5	20500 - 70600	-7.9 ± 0.3
7.0	16800 - 49000	-8.1 ± 0.2
6.4	13300 - 45700	-8.3 ± 0.2
5.8	10000 - 24900	-11.5 ± 0.5
5.3	7600 - 22100	-11.2 ± 0.3
4.9	6100 - 7500	-5 6*
4.9	7500 - 21000	-10.6 ± 0.6
4.5	4800 - 7500	-5.6 ± 0.6
4.5	7500 - 13900	-8.7 ± 0.6

* Assumed from spectra taken at $L = 4.5$.

data. The general increase in flux with decreasing distance is reflected in the increase in the counting rate observed in both the CRS data [*Gehrels et al.*, 1981] and the HIC data (Figure 1) as the spacecraft move from L values of 8 to 7.

In Figure 5, CRS and HIC spectra for oxygen and sulfur at 5.3 R_J are shown. The spectral index of the CRS oxygen data is similar to that observed below the apparent break in the HIC oxygen spectra obtained at 4.5 R_J. The position of the break in Figure 3 corresponds to ~ 13 MeV/nucleon, coincident with the maximum energy of the CRS data. To estimate the Galileo spectrum at $L = 5.3$ for energies less than 14 MeV/nucleon, we have assumed the spectral shape observed at $L = 4.5$ is typical; that is, a spectral break would be evident in the $L = 5.3$ Galileo spectrum if data were obtained at lower magnetic moments. Thus we have normalized the Galileo spectrum at $L = 4.5$ to that at $L = 5.3$ in the overlapping interval $7500 \leq \mu \leq 9000$ MeV/Gauss. As shown in Figure 5, this estimate indicates that the fluxes observed by Galileo are depleted relative to those of Voyager at the same energy/nucleon by a factor of ~ 6. Such a reduction could be due to a decrease in the diffusion rate and/or an increase in the loss rates. Because of the much lower sulfur fluxes at $L = 4.5$, a similar extrapolation to $L = 5.3$ for comparison with Voyager is not possible.

5. Phase Space Density

Phase space density is related to the quantity $J_\perp/B^2$ in the following manner:

$$f = \frac{\gamma}{2m\mu^2}\frac{J_\perp}{B^2} \quad (1)$$

where $J_\perp$ is the integral flux at a pitch angle of 90°, μ is the magnetic moment, and $\gamma = -[d\ \log(J_\perp)]/[d\ \log(\mu)]$ [*Gehrels et al.*, 1981]. To compare the HIC data with the CRS phase space density results, the pitch angle distribution of the ions and the magnetic field magnitude must be known. Galileo is a

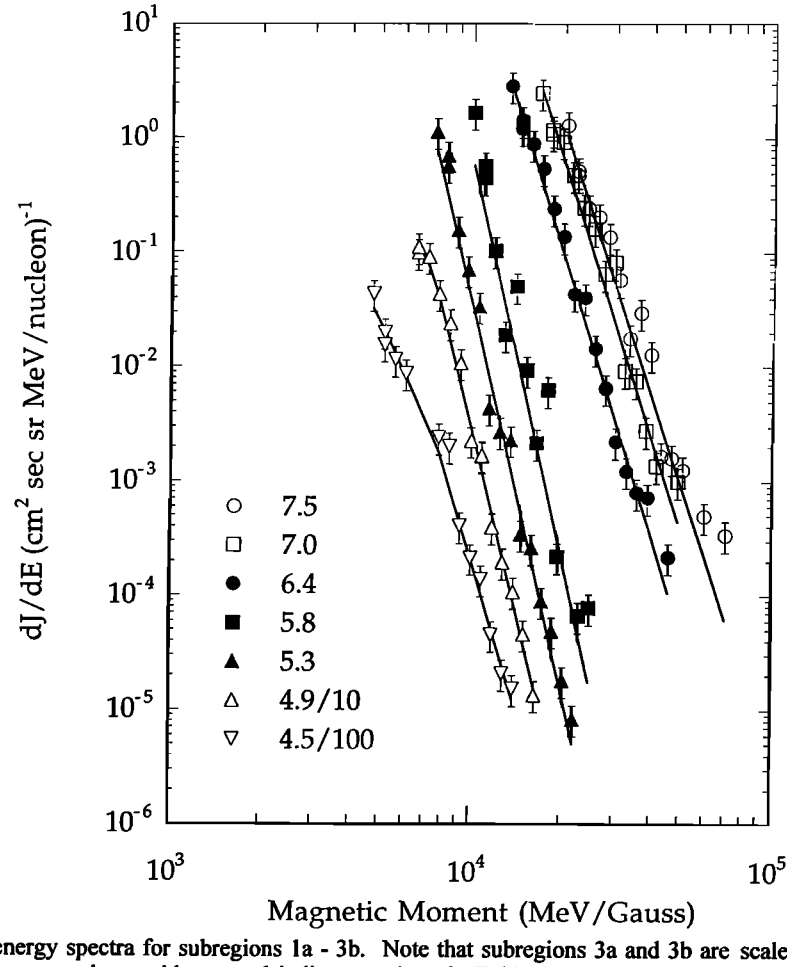

Figure 3. Oxygen energy spectra for subregions 1a - 3b. Note that subregions 3a and 3b are scaled by 10 and 100, respectively. Fits are power laws with spectral indices as given in Table 2.

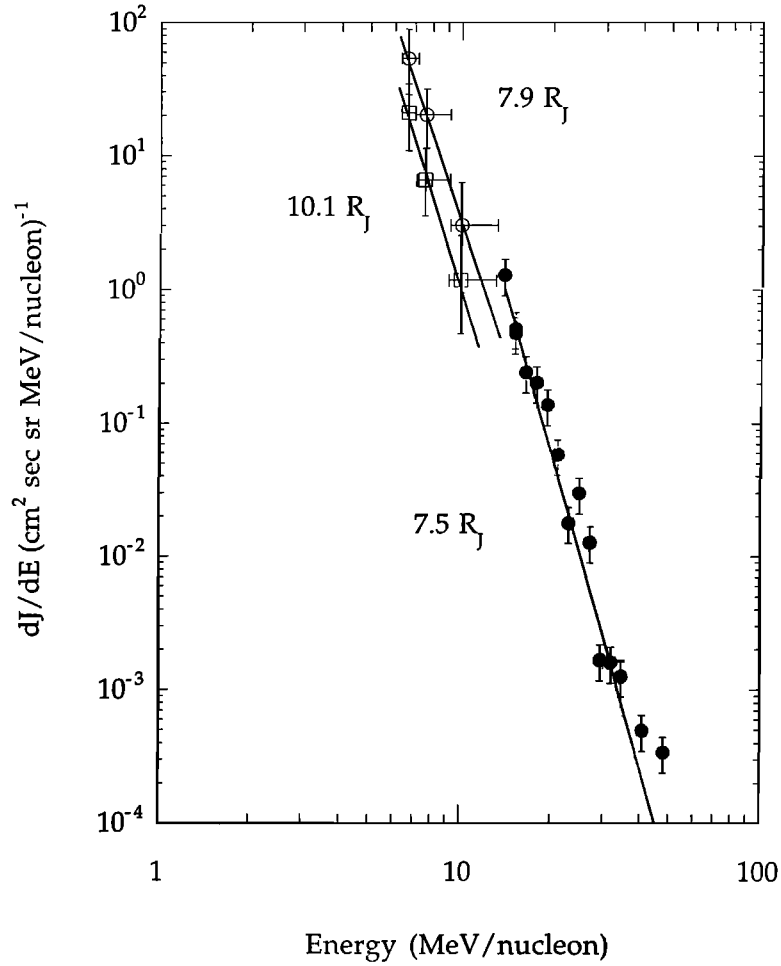

Figure 4. Oxygen energy spectra for cosmic ray subsystem (CRS) data (open squares and circles) taken at 10.1 and 7.9 R_J and heavy ion counter (HIC) data (solid circles) taken at 7.5 R_J. Fits are power laws with indices 7.0 ± 2.6 for the CRS data and 7.9 ± 0.3 for the HIC data.

spinning spacecraft and HIC is mounted such that the openings of the telescopes sweep through a plane whose normal is typically perpendicular to the direction of the magnetic field. Thus all pitch angles are sampled. The LET B rate data for 10 separate time periods during the Io pass have been accumulated as a function of spin phase. The resulting distributions have been fit with a distribution of the form given by *Gehrels* [1982]:

$$J(\alpha) \propto a_0 - \frac{a_2}{2} + \frac{3}{2} a_2 \cos^2 \alpha \tag{2}$$

where α is the pitch angle, a_2 and a_0 are fit parameters. In all 10 periods a value of a_2/a_0 = -0.21 ± 0.05 adequately represents the data.

The fluxes obtained from the HIC data also have to be converted to the fluxes expected at the magnetic equator. This is done using the fact that particles along the same magnetic field line can be related by

$$\sin^2 \alpha = \frac{B}{B_0} \sin^2 \alpha_0 \tag{3}$$

where the subscript 0 refers to values at the equator. This relation is derived from conservation of energy and magnetic moment. This, combined with the pitch angle correction, leads to

$$J_\perp = \langle J \rangle \frac{\left(1 - \frac{a_2/a_0}{2}\right)\Omega}{\left[\left(1 + \frac{a_2/a_0}{4}\right)\Omega + \frac{3}{8}\frac{a_2}{a_0}\sin\Omega\right]} \tag{4}$$

where <J> is the spin-averaged flux obtained from the HIC data and

$$\Omega = \sin^{-1}\sqrt{\frac{B_0}{B}} \tag{5}$$

Kivelson et al. [1996] have noted that the magnetic field is distorted in a region near Io. Since the duration of this deviation is small compared to the integration times used in this paper, we have not corrected for this.

At several values of the magnetic moment, a ratio of $J_\perp/B^2$ at different radial distances can be calculated and used to extend phase space density calculations made with CRS data. In Figure 6 the HIC points are given as solid symbols and the CRS data as open symbols. For $L > 6$, the CRS and HIC data are consistent, indicating little change in the ion density in this region. In contrast, *Mauk et al.* [1998] find a decrease of

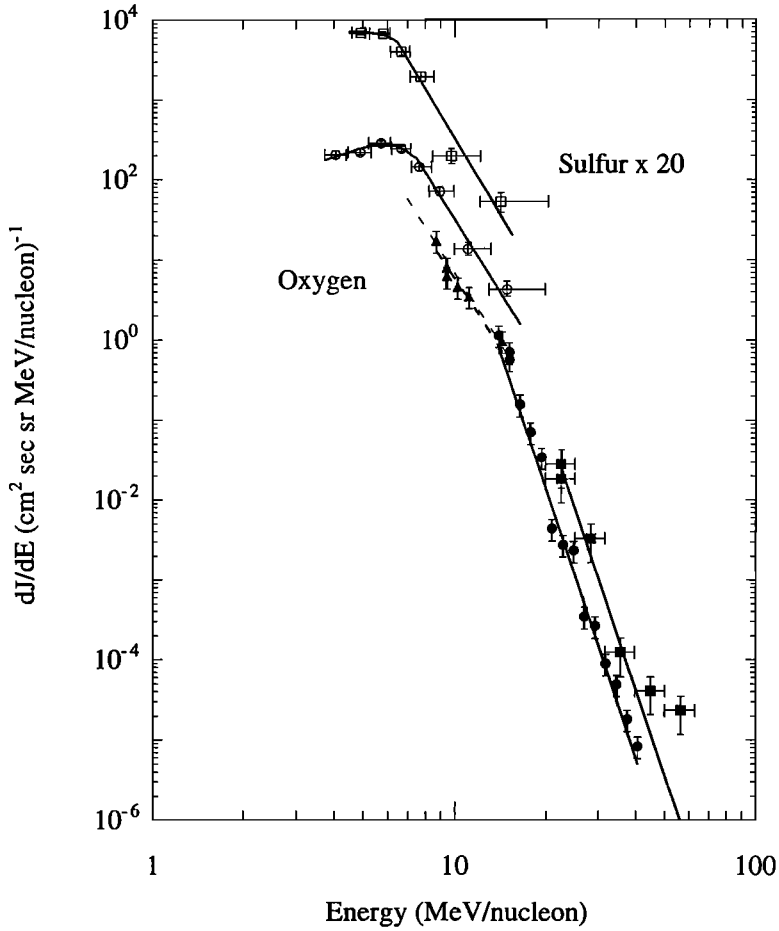

Figure 5. Oxygen and sulfur energy spectra taken at 5.3 R_J for CRS data (open circles and squares) and HIC data (solid circles and squares). HIC data from 4.5 R_J (solid triangles) have been normalized to the 5.3 R_J spectrum at 14 MeV/nucleon for comparison with the CRS oxygen spectrum. Fits are power laws.

~3 in the ion population observed at tens of kiloelectron volts by the energetic particle detector (EPD) on Galileo as compared to the low energy charged particle (LECP) instrument on Voyager. They also find that the characteristic energy of the Galileo EPD ion spectra is higher than that observed by the Voyager LECP instrument, consistent with a larger depletion at low energies than at high. Mauk et al. suggest that the depletion is caused by increased losses due to charge exchange with a neutral population denser than that observed in the time of Voyager. They point out that the cross section for these losses is strongly energy dependent with lower energies being preferentially depleted. Thus we would expect a smaller reduction at the energies measured by HIC and CRS.

The Galileo data obtained inside $L = 6$ are substantially lower than those of Voyager. Most of the difference is due to the large density gradient evident in the HIC data over roughly $5.3 < L < 6.4$, a region dominated by Io and the plasma torus. For $L < 5.3$, the density gradients observed by HIC are not very different from those seen by CRS. Because of the large averaging intervals used, the extent in L of the steep gradients cannot be accurately determined from the phase space density data. Greater radial resolution is provided by the LET E counting rate (Figure 1) which is a measure mainly of the integral flux ($J(>E)$) of oxygen with energies greater than 15 MeV/nucleon. In the absence of losses the integral flux should increase with decreasing L according to $J(>E) \sim L^{-(3\gamma+6)}$ due to inward diffusion and betatron acceleration. As seen in Figure 1b, there is an Io absorption microsignature at $6.0 \geq L \geq 5.9$. That the radial profile is slowly increasing just inside Io at $5.9 \geq L \geq 5.73$ and only modestly increasing into $L = 5.61$ indicates significant losses occur between $L \sim 5.6$ and ~ 5.9. Much smaller losses at $L < 5.61$ result in a rapidly increasing flux with decreasing L, consistent with the smaller radial gradients in phase space density shown in Figure 6 for $L \leq 5.3$.

Richardson and Siscoe [1981] pointed out that the sharp inner edge of the Io plasma torus indicated a much smaller radial diffusion coefficient inside than outside Io's orbit where centrifugal interchange instabilities are effective. This results in a small inward diffusion velocity and longer times for losses to reduce the phase space density [e.g., *Thorne*, 1982]. While this corresponds to the same L region where the large Galileo gradient was observed, the difference in the magnitude of the gradient as observed by Galileo compared to that of Voyager remains to be explained.

Galileo passed much closer to Io (900 km) than Voyager (20570 km); however, it is unlikely that this explains the difference in observed gradients since the distance from the moon should only affect the particle density within the

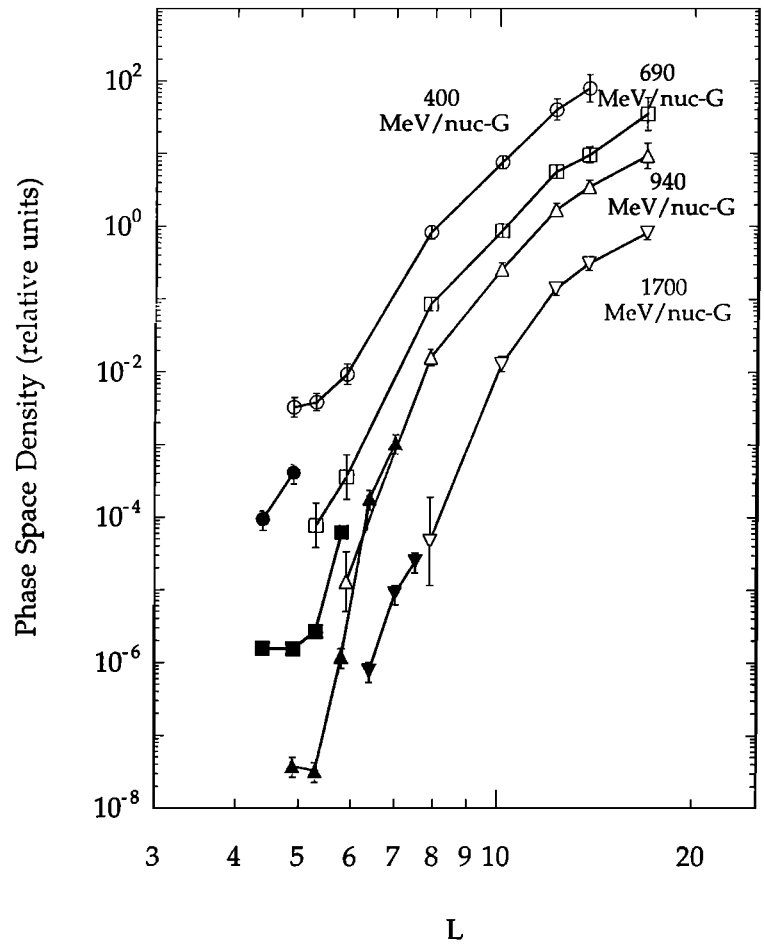

Figure 6. Phase space density as a function of L value for several different magnetic moments. Open symbols are CRS data; solid symbols are HIC data.

microsignature (seen in the Galileo data at L = 5.9 – 6.0), certainly not over a region as large as L = 5.6 - 5.9. It can be seen from Figure 7 that the Galileo and Voyager data for $L \geq$ 5.3 were obtained at different local times. *Armstrong et al.* [1981] observed a significant inbound-outbound asymmetry in the ion fluxes measured near Io's orbit, possibly due to local time differences. Similarly, the discrepancy between the Galileo and Voyager phase space densities could be a result of the ~ 6 hour local time difference, although the data presented by *Gehrels and Stone* [1983] from L = 5.9 – 5.3 are averaged over two periods separated by ~ 3 hours in local time. Alternatively, the larger losses observed by Galileo could indicate that either radial diffusion was slower or scattering timescales were shorter than at the time of the Voyager observations.

6. Conclusions

The HIC sensor on Galileo is very similar to the CRS instrument on Voyager yet covers a larger energy range and has a bigger geometric factor. Thus combining the data allows a more complete picture to be made of the properties of the high-energy particles found in the inner magnetosphere of Jupiter. Such a comparison was made using the Galileo encounter with Io upon the spacecraft arrival at Jupiter and the CRS data presented by *Gehrels and Stone* [1983].

The comparison for L ~ 7.5 to 10 indicates that the oxygen spectrum is consistent with a single power law of γ ~ -8 above ~ 6 MeV/nucleon. Combining the data inside L = 6 suggests that there is a break in the spectrum at ~ 13 MeV/nucleon. The position of this break is consistent with that seen in the Galileo oxygen spectra obtained at 4.5 R_J (and hinted at in the L = 4.9 data) and corresponds to an oxygen gyroradius of ~ 1.5 R_{Io}, implying that Io more efficiently absorbs ions with gyroradii less than this.

Oxygen spectra obtained outside the orbit of Io are substantially harder than those acquired inside. There is a slight decrease in the spectral index as L decreases toward Io which is expected in the presence of significant strong pitch angle scattering. The distinct change in index from outside to inside the Io orbit is consistent with a dramatic change in the diffusion time near L = 6. The spectral indices obtained at L < 6 suggest that particle scattering at the strong pitch angle scattering limit is not the dominant loss process in this region although significant scattering losses are still occurring.

Calculations of J_1/B^2 allow the phase space density curves of *Gehrels and Stone* [1983] to be extended to smaller L values for four values of the magnetic moment. For L > 6 the densities observed by HIC and CRS are comparable, while at smaller distances the HIC densities are substantially reduced. In the L range of 5.6-5.9, significant losses are occurring, similar to a region at the inner edge of the plasma torus

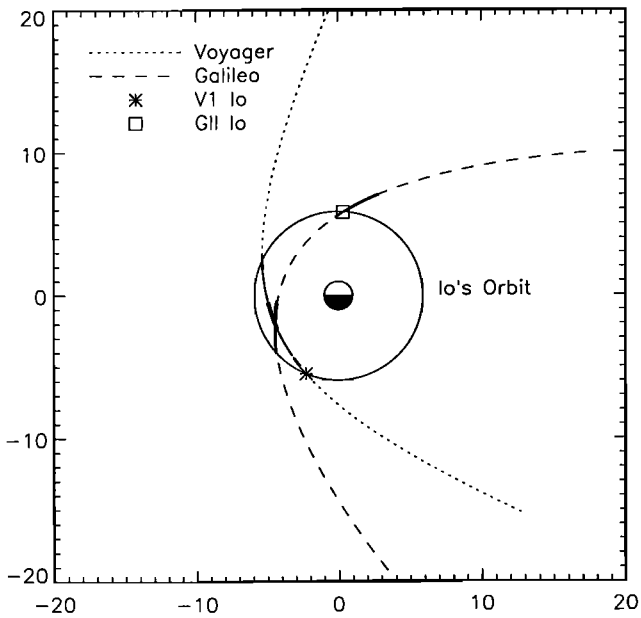

Figure 7. Orbits of Galileo (dashed line) and Voyager 1 (dotted line), where a longitude offset has been applied to align the Sun occultation zones for each pass to illustrate local time differences. The Galileo-Io encounter is indicated by the square. The Voyager-Io encounter is indicated by the asterisk. The solid lines on the Galileo trajectory indicate where HIC data were accumulated for this work. The solid line sections of the Voyager orbit correspond to CRS data obtained at 5.9 (thick line), 5.3 (thin line) and 4.9 (thicker line) R_J.

examined by *Richardson and Siscoe* [1981] using Voyager plasma data but to a larger degree than observed by Voyager. This difference could be the result of local time asymmetries or a decrease in the diffusion rate and/or scattering timescales.

Acknowledgments. Janet G. Luhmann thanks both referees for theis assistance in evaluating this paper.

References

Armstrong, T.P., M.T. Paonessa, S.T. Brandon, S.M. Krimigis, and L.J. Lanzerotti, Low-energy charged particle observations in the 5 – 20 R_J region of the Jovian magnetosphere, *J. Geophys. Res., 86,* 8343, 1981.

Barbosa, D.D., A. Eviatar, and G.L. Siscoe, On the acceleration of energetic ions in Jupiter's magnetosphere, *J. Geophys. Res., 89,* 3789, 1984.

Garrard, T.L., N. Gehrels, and E.C. Stone, The Galileo heavy element monitor, *Space Sci. Rev., 60,* 305, 1992.

Garrard, T.L., E.C. Stone, and N. Murphy, Effects of absorption by Io on composition of energetic heavy ions, *Science, 274,* 393, 1996.

Gehrels, N., and E.C. Stone, Energetic oxygen and sulfur ions in the Jovian magnetosphere and their contribution to the auroral excitation, *J. Geophys. Res., 88,* 5537, 1983.

Gehrels, N., E.C. Stone, and J.H. Trainor, Energetic oxygen and sulfur in the Jovian magnetosphere, *J. Geophys. Res., 86,* 8906, 1981.

Hamilton, D.C., G. Gloeckler, A.B. Galvin, J. Geiss, and R. von Steiger, The charge states of oxygen ions observed in the magnetosphere of Jupiter with SWICS on Ulysses, *Eos Trans. AGU 73,* 181, 1992.

Kivelson, M.G., K.K. Khurana, R.J. Walker, J. Warnecke, C.T. Russell, J.A. Linker, D.J. Southwood, and C. Polanskey, Io's interaction with the plasma torus: Galileo magnetometer report, *Science, 274,* 396, 1996.

Krimigis, S.M., et al., Low energy charged particle environment at Jupiter, a first look, *Science, 204,* 998, 1979a.

Krimigis, S.M., et al., Hot plasma environment at Jupiter: Voyager 2 results, *Science, 206,* 977, 1979b.

Mauk, B.H., et al., Galileo-measured depletion of near-Io hot ring current plasmas since the Voyager epoch, *J. Geophys. Res., 103,* 4715, 1998.

Richardson, J.D., and G.L. Siscoe, Factors governing the ratio of inward to outward diffusing flux of satellite ions, *J. Geophys. Res., 86,* 8485-8490, 1981.

Siscoe, G.L., A. Eviatar, R.M. Thorne, J.D. Richardson, F. Bagenal, and J.D. Sullivan, Ring current impoundment of the Io plasma torus, *J. Geophys. Res., 86,* 8480-8484, 1981.

Stone, E.C., R.E. Vogt, F.B. McDonald, B.J. Teegarden, J.H. Trainor, J.R. Jokipii, and W.R. Webber, Cosmic ray investigation for the Voyager missions: Energetic particle studies in the outer heliosphere - and beyond, *Space Sci. Rev., 21,* 35, 1977.

Thorne, R.M, Injection and loss mechanisms for energetic ions in the inner Jovian magnetosphere, *J. Geophys. Res., 87,* 8105, 1982.

Vogt, R.E., et al., Voyager 1: Energetic ions and electrons in the Jovian magnetosphere, *Science, 204,* 1003, 1979a.

Vogt, R.E., et al., Voyager 2: Energetic ions and electrons in the Jovian magnetosphere, *Science, 206,* 984, 1979b.

C.M.S. Cohen, T.L. Garrard, and E.C. Stone, Space Radiation Laboratory, California Institute of Technology, MC 220-47, Pasadena, CA 91125. (cohen@srl.caltech.edu).

J.F. Cooper, Hughes STX Corporation, Space Physics Data Facility, MC 632, NASA/Goddard Space Flight Center, Greenbelt, MD 20771.

N. Murphy, Jet Propulsion Laboratory, MS 169-506, 4800 Oak Grove Dr., Pasadena, CA 91109.

N. Gehrels, MC661, NASA/Goddard Space Flight Center, Greenbelt, MD 20771.

(Received January 21, 1999; revised December 1, 1999; accepted December 1, 1999.)